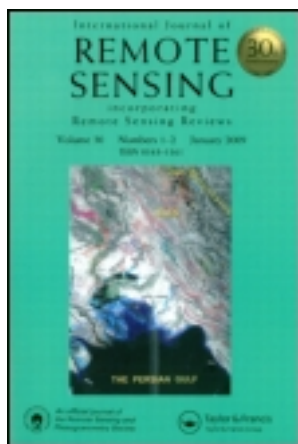


This article was downloaded by: [West Virginia University]

On: 13 February 2014, At: 12:54

Publisher: Taylor & Francis

Informa Ltd Registered in England and Wales Registered Number: 1072954 Registered office: Mortimer House, 37-41 Mortimer Street, London W1T 3JH, UK



## International Journal of Remote Sensing

Publication details, including instructions for authors and subscription information:

<http://www.tandfonline.com/loi/tres20>

### Mapping vegetation morphology types in a dry savanna ecosystem: integrating hierarchical object-based image analysis with Random Forest

Niti B. Mishra<sup>a</sup> & Kelley A. Crews<sup>a</sup>

<sup>a</sup> Department of Geography & the Environment, The University of Texas, 1 University Station, A3100, Austin, TX 78712, USA

Published online: 13 Feb 2014.

To cite this article: Niti B. Mishra & Kelley A. Crews (2014) Mapping vegetation morphology types in a dry savanna ecosystem: integrating hierarchical object-based image analysis with Random Forest, International Journal of Remote Sensing, 35:3, 1175-1198, DOI: [10.1080/01431161.2013.876120](https://doi.org/10.1080/01431161.2013.876120)

To link to this article: <http://dx.doi.org/10.1080/01431161.2013.876120>

PLEASE SCROLL DOWN FOR ARTICLE

Taylor & Francis makes every effort to ensure the accuracy of all the information (the "Content") contained in the publications on our platform. However, Taylor & Francis, our agents, and our licensors make no representations or warranties whatsoever as to the accuracy, completeness, or suitability for any purpose of the Content. Any opinions and views expressed in this publication are the opinions and views of the authors, and are not the views of or endorsed by Taylor & Francis. The accuracy of the Content should not be relied upon and should be independently verified with primary sources of information. Taylor and Francis shall not be liable for any losses, actions, claims, proceedings, demands, costs, expenses, damages, and other liabilities whatsoever or howsoever caused arising directly or indirectly in connection with, in relation to or arising out of the use of the Content.

This article may be used for research, teaching, and private study purposes. Any substantial or systematic reproduction, redistribution, reselling, loan, sub-licensing, systematic supply, or distribution in any form to anyone is expressly forbidden. Terms &

Conditions of access and use can be found at <http://www.tandfonline.com/page/terms-and-conditions>

## Mapping vegetation morphology types in a dry savanna ecosystem: integrating hierarchical object-based image analysis with Random Forest

Niti B. Mishra\* and Kelley A. Crews

Department of Geography & the Environment, The University of Texas, 1 University Station, A3100,  
Austin, TX 78712, USA

(Received 22 April 2013; accepted 30 November 2013)

Savanna ecosystems are geographically extensive and both ecologically and economically important, and require monitoring over large spatial extents. Remote-sensing-based characterization of vegetation properties in savannas is methodologically challenging, mainly due to high structural and functional heterogeneity. Recent advances in object-based image analysis (OBIA) and machine learning algorithms offer new opportunities to address these challenges. Focusing on the semi-arid savanna ecosystem in the central Kalahari, this study examined the suitability of a hierarchical OBIA approach combined with *in situ* data and an ensemble classification technique for mapping vegetation morphology types at landscape scale. A stack of Landsat TM imagery, NDVI, and topographic variables was segmented with six different scale factors resulting in a hierarchical network of image objects. Sample objects for each vegetation morphology class were selected at each segmentation scale and classification was performed using optimal features consisting of spectral and textural features. Overall and class-specific classification accuracies were compared across the six scales to examine the influence of segmentation scale on each. Results suggest that the highest overall classification accuracy (i.e. 85.59%) was observed not at the finest segmentation scale, but at coarse segmentation. Additionally, individual vegetation morphology classes differed in the segmentation scale at which they achieved highest classification accuracy, reflecting their unique ecology and physiognomic composition. While classes with high vegetation density/height attained higher accuracy at fine segmentation scale, those with lower vegetation density/height reached higher classification accuracy at coarse segmentation scales. Contrarily, for pans and bare areas, accuracy was relatively unaffected by changing segmentation scale. Variable importance plots suggested that spectral features were the most important, followed by textural variables. These results show the utility of the OBIA approach and emphasize the requirement of multi-scale analysis for accurately characterizing savanna systems.

### 1. Introduction

Savanna ecosystems are mixed tree-grass systems that cover over 40% of the global terrestrial area (50% of Africa) and play a significant role in the global land–atmosphere energy balance as well as carbon and nutrient cycles (Mistry 2000; Hill, Roman, and Schaaf 2011). Especially in southern Africa, savannas are essential contributors to productivity and biodiversity and also contain some of the largest remaining wildlife habitats (Scholes and Walker 1993). Vegetation structure and landscape composition in savanna systems is characterized as patchy, mainly as a result of high spatio-temporal variability in

---

\*Corresponding author. Email: [niti@mail.utexas.edu](mailto:niti@mail.utexas.edu)

rainfall and fire history (Turner et al. 2003; Wiegand, Saltz, and Ward 2006). Besides providing ecosystem goods and services, southern African savannas are also economically significant as they offer the basis of economic activity by supporting high populations of livestock as well as wildlife-based tourism (Werger 1973; Thomas and Sporton 1997). Over the past two decades, many areas in the southern Africa savanna in general and the central Kalahari region in particular have become the focus of attention of stakeholders and government. These areas are perceived as large, untapped grazing resources with the potential of pastoral agriculture that can be a source of both people's livelihoods and government revenue (Skarpe 1990; Thomas and Sporton 1997; Dougill, Thomas, and Heathwaite 1999; Thomas and Twyman 2004). As a result, large parts of previously wild and undisturbed areas are experiencing structural and functional changes in vegetation characteristics, mainly due to changing land use, and altered fire regimes exacerbated by climatic shifts (Werger 1973; Turner et al. 1993; Dougill, Thomas, and Heathwaite 1999; Scholes et al. 2002). These changes are in turn affecting biogeochemical processes, availability of habitat-related key structural resources (e.g. solitary nesting trees, foraging grounds, and migration routes), and the overall ecological sustainability (Dougill, Thomas, and Heathwaite 1999; Tews, Blaum, and Jeltsch 2004; Blaum, Rossmanith, and Jeltsch 2007).

Sustainability of these fragile and dynamic systems needs ecologically informed decision-making by land managers who require fundamental knowledge about the functional attributes of vegetation assemblages (e.g. vegetation structure, cover, density). These characteristics are also key variables in state and transition models used for modelling these systems (Van Rooyen et al. 1990; Scholes and Walker 1993). However, countries in southern Africa lack such geodata on vegetation and land cover at suitable spatial scales. Field-based assessment, though of high quality, is limited in scope and scale, especially considering systems that are extensive and wild. Further, vegetation dynamics is the result of processes interacting at multiple spatial scales that require monitoring at local to regional scales (Cramer et al. 2001; Xie, Sha, and Yu 2008). Remote-sensing instruments provide valuable tools for this purpose and can not only complement field measurements but also provide much larger spatial coverage (Elmore et al. 2000; Wu and Marceau 2002). With the increasing number of remote-sensing systems, images are available at multiple spatial scales, but with trade-off between spatial resolution, temporal resolution, and swath area. Systems providing low-spatial resolution images (>250 m, e.g. MODIS) have high temporal revisit and large swath area, making them more suitable for regional-scale monitoring. While coarse-resolution images have been able to yield high accuracy in ecosystems with homogeneous cover, they have been found to produce much lower accuracy and high uncertainty in savanna systems, mainly due to small patch size and heterogeneous classes with mixed vegetation (Latifovic and Olthof 2004; Turner et al. 2004; Giri, Zhu, and Reed 2005, Mishra, Crews, and Okin under review). Contrarily, very high-spatial resolution imagery (<10 m) provides the required spatial detail but is limited by small swath area, large data volume, low temporal frequency, and high data cost. Medium-spatial resolution imagery (20–30 m) (e.g. Landsat, ASTER) represents a good compromise in this regard and has been favoured for landscape-level applications in savanna systems (Ringrose et al. 2003; Schwartz et al. 2003; Seagle 2003; Davidson et al. 2008; Tangestani et al. 2008). Compared with low-spatial-resolution imagery, results obtained with medium-resolution imagery are ecologically more meaningful as these allow one to infer landscape patterns and related ecological processes (Opdam, Foppen, and Vos 2002; Newton et al. 2009). However, in semi-arid savannas, inferring vegetation properties from medium-resolution imagery is

also methodologically challenging for several reasons, e.g. expansive soil background leading to swamping out of spectral contribution of plants, lack of a strong red edge, and reduced absorption in visible wavelengths due to evolutionary adaptations of semi-arid vegetation (Huete, Jackson, and Post 1985; Huete and Jackson 1988; Okin et al. 2001; Wu and Marceau 2002).

Since savanna systems are often considered patch-dynamic systems, mapping vegetation properties in savannas may benefit from object-based image analysis (OBIA) rather than the traditional per-pixel analysis approach (Spies, Ripple, and Bradshaw 1994; Soranno et al. 1999; Steffan-Dewenter et al. 2002; Laliberte et al. 2004). Following the OBIA approach, imagery is first segmented into objects representing a relatively homogeneous group of pixels by selecting desired scale, shape, and compactness criteria. Segmentation is followed by sample selection and classification of segments into classes of interest (Steffan-Dewenter et al. 2002; Benz et al. 2004). In savanna systems, important OBIA advantages include (1) treatment of landscape consisting of relatively homogeneous patches (or 'objects') is ecologically more suitable than individual pixels; (2) landscape patches often depict scale dependency and, following the OBIA approach, landscape objects can be generated at multiple segmentation scales that can provide added insight into ecological processes (Strayer et al. 2003); (3) lower likelihood of 'salt-and-pepper' speckle, which is often an issue with per-pixel analysis; and (4) OBIA offers the opportunity to add contextual, geometrical, and texture related features (Strayer, Ewing, and Bigelow 2003). However, the OBIA approach has not yet been extensively tested in natural landscapes where continuous variation in vegetation characteristics makes it challenging to define boundaries between 'objects' (Soranno et al. 1999; Tallmon et al. 2003).

Unlike human-modified landscapes (e.g. urban areas), in heterogeneous natural systems, landscape patches can vary in size, shape, and structure that may require characterization at multiple spatial scales (Moustakas et al. 2009, Mishra and Crews 2013). Within OBIA, the segmentation scale parameter used in segmentation controls the maximum allowable object-level spectral heterogeneity and object size (Urban et al. 2002). Scale also affects the quality of segmented objects, which in turn affects the final classification accuracy (Keyghobadi, Roland, and Strobeck 1999; Yu et al. 2006). By manipulating the segmentation scale factor, nested objects of different size can be created that could be further hierarchically classified representing the output at multiple scales. While such a hierarchical classification approach has been found appropriate for characterizing spatially heterogeneous natural systems such as wetlands (Trzcinski, Fahrig, and Merriam 1999) and arid rangelands, its suitability for characterizing vegetation morphology in dry savanna systems at the landscape scale merits further investigation.

Determining suitable classification feature space is a crucial step before image classification, which ensures that the classes in question are discriminated effectively and with sufficiently high accuracy (Knight and Morris 1996). Following OBIA, the availability of hundreds of features (e.g. spectral, geometrical, textural, and contextual) makes it a time-consuming and subjective process (Turner 1989). Specifically, the inclusion of textural features in OBIA increases the processing time significantly, thus limiting its suitability for landscape-scale mapping (Soranno et al. 1999). Very few previous studies have examined which classification features are more appropriate for characterizing vegetation morphology in xeric systems. Additionally, in low-niche differentiation environments such as the semi-arid savannas, separability of vegetation classes and classification accuracy may be enhanced by using more recently proposed non-parametric classification algorithms (e.g. classification trees). The application of ensemble of classification trees

(i.e. Random Forest, RF), as proposed by Breiman (2001), has been proved to be effective for classifying remotely sensed data. Remote-sensing studies utilizing RF classification have focused on the per-pixel classification approach and regional- to global-scale studies. More recently, their application under the OBIA approach has been found to enhance thematic depth and classification accuracy. Therefore, this study explored the utility of OBIA combined with RF classification for mapping vegetation morphology types in the semi-arid central Kalahari of Botswana. The study area is relatively understudied and lacks landscape-scale environmental geodata due to accessibility and the dangers from wildlife. The primary objective of this study was to utilize *in situ* information on vegetation physiognomic characteristics to develop and map vegetation morphology types using OBIA by determining the optimal segmentation scale and classification features.

## 2. Site and situation

Part of the southern African semi-arid savanna system, the central Kalahari (between 21°–24° S and 22°–26° E) occupies the northern and central part of the larger Kalahari sand basin. The area follows the Kalahari rainfall gradient, with its northern and the western tips receiving up to 400 mm of rainfall whereas the rest of the area receives a mean annual precipitation of 350 mm. The rainy season is between October and April, during which rainfall is spatially discontinuous and temporally variable (Makhabu, Marotsi, and Perkins 2002; Scholes et al. 2002). The study area covers 22,292 km<sup>2</sup>, of which more than 70% falls within the protected area (i.e. the Central Kalahari Game Reserve) and the rest is under private game farms and open-access commercial ranching (Figure 1). Geologically, the area is dominated by the spread of nutrient-poor Kalahari sand with sporadic outcrops of calcrete, sandstone, and schist of the Karoo sequence, with an average altitude of 950 m (Fagan 2002). The topographical continuity is broken in the northern part of the study area due to the existence of longitudinal dune systems marked by comparatively much higher and denser vegetation. The natural water availability is limited to small, short-lived accumulations in occasional pan depressions (Dougill and Trodd 1999). The vegetation is characterized by a spatially complex and structurally heterogeneous mixture of woody and herbaceous species occurring on a scale of few metres, and exhibits temporally distinct phenological patterns. Notable broad-leaved species in the area include *Lonchocarpus nelsii*, *Terminalia sericea*, *Bauhinia petersiana*, *Combretum hereroense*, and *Croton gratissimu*. Important fine-leaved species include *Acacia erioloba*, *A. luederitzii*, *A. mellifera*, *A. erubescens*, and *Ziziphus mucronata* (Fagan 2002). Plant species diversity is relatively low for all plant communities and the differences among communities are related to changes in species dominance rather than occurrence of different species. Thus, vegetation boundaries based on plant species are often unclear (Fagan 2002; Makhabu, Marotsi, and Perkins 2002). As in much of southern Africa's savannas, pans are geomorphologically distinct features with relatively flat topography and clay-dominated soil. Pans are different from other bare areas in that they are mostly contained within isolated sub-circular to sub-elliptical depressions that retain rain water for much longer. In the study area, many pans (e.g. Deception pan, Lethiahau pan) are remnants of ancient sand-choked drainage lines (also called fossil river valleys). Pans are ecologically important as they provide mineral licks and relatively nutrient-rich vegetation, attracting large herbivores and their associated predators and concomitant tourism (Turner 2005). Therefore, accurate mapping of pan areas is important for the overall planning and management of the central Kalahari region.

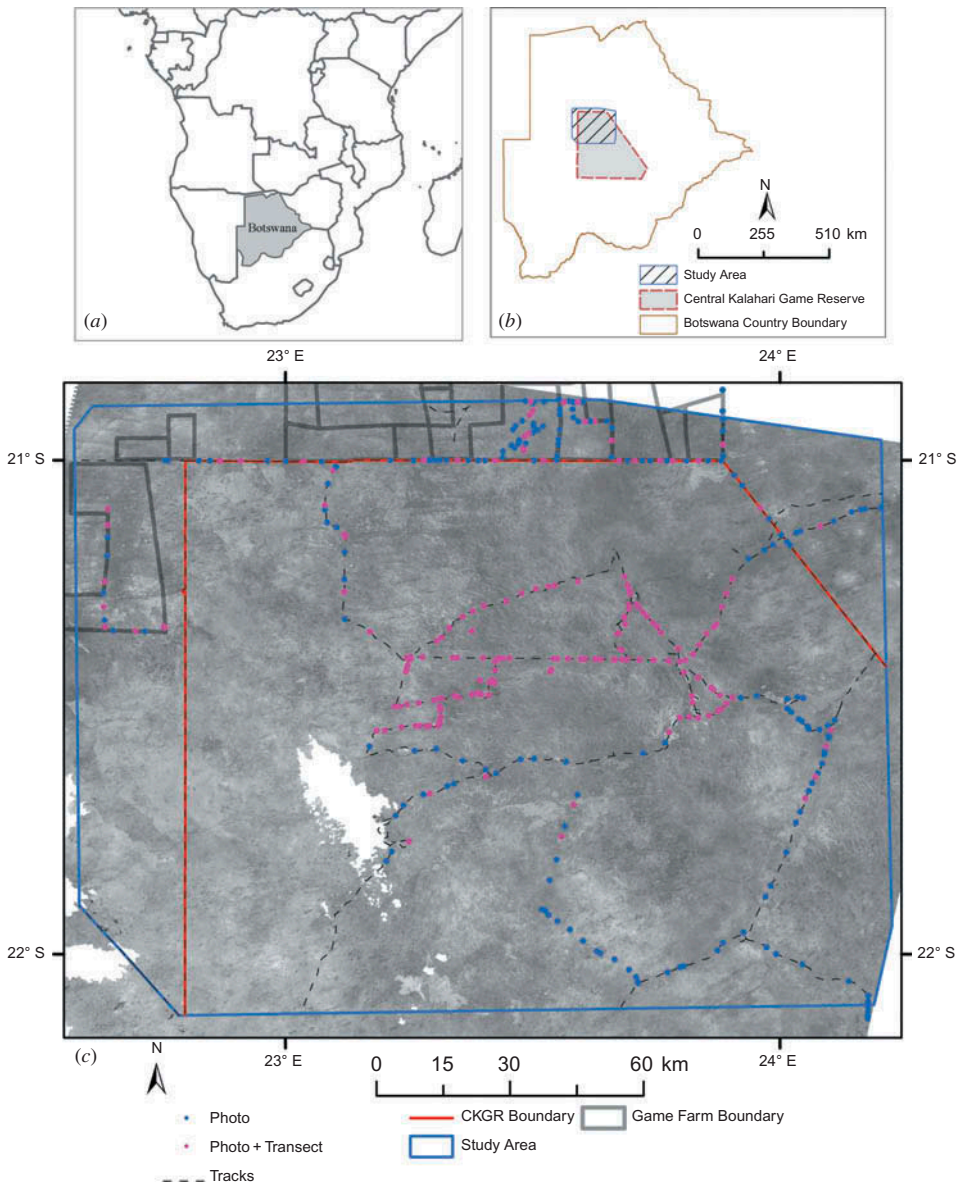


Figure 1. (a) Location of Botswana in southern Africa; (b) location of the study area in the central Kalahari of Botswana; and (c) enlarged portion of the study area depicting the game reserve boundary and game farms outside the protected area; the points are where field data were collected. The background image used in this study is cloud-masked Landsat TM (band 4).

### 3. Data and methods

#### 3.1. Remotely sensed data and pre-processing

This study used terrain-corrected (Level 1T) Landsat 5 TM imagery acquired at 10:16 local time (08:16 UTC) on 9 May 2010. In the central Kalahari, May represents the beginning of the dry season when trees and shrubs are still green, whereas herbaceous

vegetation contains no observable green biomass. Clouds in this imagery were manually masked and surface reflectance was derived by radiometrically calibrating the imagery using the ATCOR algorithm. ATCOR is an absolute atmospheric correction method that applies an atmospheric look-up table based on a large database containing the results of radiative transfer calculation from the MODTRAN-4 radiative transfer code (Pearson, Turner, and Drake 1999). The optical depth of the atmospheric aerosols was calculated by comparing modelled at-sensor radiance to measured radiance in the red band of areas with dark, dense vegetation. This correction was then applied on each pixel to derive surface reflectance. As an additional feature, the normalized difference vegetation index (NDVI) was derived after calibrating Landsat TM imagery. An ASTER GDEM (Version 2) representing the study area was also used to derive slope and aspect. At high spatial resolution, GeoEye-1 and SPOT-5 images were available covering 1353 km<sup>2</sup> (6%) and 15,821 km<sup>2</sup> (70%) of the study area, respectively.



### 3.2. Field data processing and development of vegetation morphology classes

Field data related to vegetation physiognomy (i.e. structure and density) and species composition were acquired following a transect-based approach during two field campaigns conducted during 18 May–2 June 2011 and 11–28 May 2012 (coincident with the calendar month of image acquisition). The location of these transects was determined based on knowledge gained during a May 2010 reconnaissance trip and visual interpretation of high-spatial resolution imagery (i.e. GeoEye/SPOT). Transect locations were spatially distributed with the aim of sampling all important vegetation morphological types in the study area. Due to serious accessibility and safety issues (e.g. danger of predator attack), these transects could not be established away from tracks except in the pan and more open areas. Combining the fieldwork conducted during 2011 and 2012, data were collected from 148 transects (Figure 1). At each of these transects, geographic coordinates were recorded at the start and end points using a standard global positioning system. Additional information included visual interpretation of the dominant vegetation functional type (e.g. woody *versus* herbaceous), minimum, maximum, and average vegetation height, dominant tree/shrub species, and images acquired with a digital camera. These characteristics were also interpreted and recorded at 143 further locations where setting up a transect was not possible due to high vegetation density and serious safety issues (Figure 1).

In southern African savanna systems, at the spatial/spectral resolution of Landsat imagery, vegetation physiognomic-structural aspects are the most important determinants of pixel reflectance (Groffman et al. 2005). Hence, the development of vegetation morphology classes was based on (1) vegetation physiognomy, (2) vertical and horizontal agreement, (3) leaf type, and (4) phenology. The accurate representation of the typical co-existence of trees, shrubs, and grasses in a savanna ecosystem requires consideration of the layering system of vegetation structure. An important advantage of considering the layering system in heterogeneous systems such as savannas is the independence of geographic scale (Groffman et al. 1992). Thus, considering the layering system of vegetation and the above-mentioned physiognomic characteristics recorded in field transects, the following five vegetation morphology classes were defined: (1) mixed deciduous woodland with shrubs and herbaceous layer; (2) mixed (70–40%) medium-high shrubland with open, short herbaceous layer; (3) mixed (40–10%) medium-high shrubland with open, short herbaceous layer; (4) medium-tall grassland with medium-high shrubs; and (5) pans and bare areas (Table 1).

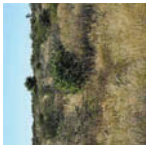




Table 1. Different vegetation morphology types and their physiognomic characteristics considered in this study as derived from field measurements.

Field Photo	Class name (main woody or herbaceous species)	No. of field transect/photo locations	Vegetation structure	Average # of objects (training/validation)
	Class 1: Mixed deciduous woodland with shrubs and herbaceous layer (species: <i>Terminalia prunioides</i> , <i>C. mopane</i> , <i>Acacia erioloba</i> , <i>Croton gratissimus</i> )	27/14	<p>First layer:</p> <ul style="list-style-type: none"> <li>Life form: trees</li> <li>Mean percentage cover: 13.4%</li> <li>Mean height: 20 m</li> </ul> <p>Second layer:</p> <ul style="list-style-type: none"> <li>Life form: shrubs</li> <li>Mean percentage cover: 41.6%</li> <li>Mean height: 6 m</li> </ul> <p>Third layer:</p> <ul style="list-style-type: none"> <li>Life form: herbaceous vegetation</li> <li>Mean percentage cover: 32%</li> <li>Mean height: 0.8 m</li> </ul>	218/87
	Class 2: Mixed (70-40%) medium high shrubland with open short herbaceous layer (species: <i>Acacia mellifera</i> , <i>Croton gratissimus</i> , <i>Acacia erubescens</i> )	59/38	<p>First layer:</p> <ul style="list-style-type: none"> <li>Life form: shrubs</li> <li>Mean percentage cover: 36.4%</li> <li>Mean height: 5.5 m</li> </ul> <p>Second layer:</p> <ul style="list-style-type: none"> <li>Life form: herbaceous vegetation</li> <li>Mean percentage cover: 46.8%</li> <li>Mean height: 0.7 m</li> </ul>	446/178

(Continued)

Table 1. (Continued).

Field Photo	Class name (main woody or herbaceous species)	No. of field transect/photo locations	Vegetation structure	Average # of objects (training/validation)
	Class 3: Mixed (40-10%) medium high shrubland with open short herbaceous layer (species: <i>L. nelsii</i> , <i>C. alexandri</i> , <i>Banhinia pelerstiana</i> , <i>G. Flava</i> )	91/54	<p>First layer:</p> <ul style="list-style-type: none"> <li>Life form: shrubs</li> <li>Mean percentage cover: 24.08%</li> <li>Mean height: 3.4 m</li> </ul> <p>Second layer:</p> <ul style="list-style-type: none"> <li>Life form: herbaceous vegetation</li> <li>Mean percent cover: 48.05%</li> <li>Mean height: 0.5 m</li> </ul>	1097/439
	Class 4: Medium tall grassland with medium high shrubs (species: <i>Stipagrostis</i> spp, <i>Aristida</i> spp, <i>L. nelsii</i> )	55/32	<p>First layer:</p> <ul style="list-style-type: none"> <li>Life form: shrubs</li> <li>Mean percentage cover: 14.11%</li> <li>Mean height: 2.6 m</li> </ul> <p>Second layer:</p> <ul style="list-style-type: none"> <li>Life form: herbaceous vegetation</li> <li>Mean percent cover: 55.36%</li> <li>Mean height: 2 m</li> </ul>	520/208
	Class 5: Pans and bare areas (species: <i>Enneapogon desvauxii</i> , <i>Sporobolus iocladus</i> )	56/23	<p>First layer:</p> <ul style="list-style-type: none"> <li>Life form: herbaceous vegetation</li> <li>Mean percentage cover: &lt;15%</li> <li>Mean height: 0.1 m</li> </ul>	1188/683

### 3.3. Object-based image analysis

#### 3.3.1. Image segmentation and training object selection

The workflow of the methodology followed in this study is outlined in Figure 2. To implement object-based classification, first, image segmentation was carried out in eCognition Developer 8 software (Loreau, Mouquet, and Holt 2003). The raster stack (six Landsat bands excluding the thermal band, NDVI, DEM, slope, and aspect) was segmented using a multi-resolution segmentation algorithm. The multi-resolution segmentation approach allows construction of objects of different size and enhances the response of object generation to landscape patch structure in comparison with other approaches (Naiman and Rogers 1997; Jules et al. 2002). Due to high structural heterogeneity in savanna systems, meaningful spectrally homogeneous objects can occur at different spatial scales (Naiman and Rogers 1997). Additionally, based on field information on landscape heterogeneity, it was expected that optimal patch size would vary depending on vegetation morphological characteristics. Hence, in this study objects were generated at six segmentation levels with scale values ranging from 15 to 60, resulting in an average object size of 20,358–408,625 m<sup>2</sup> (Table 2).

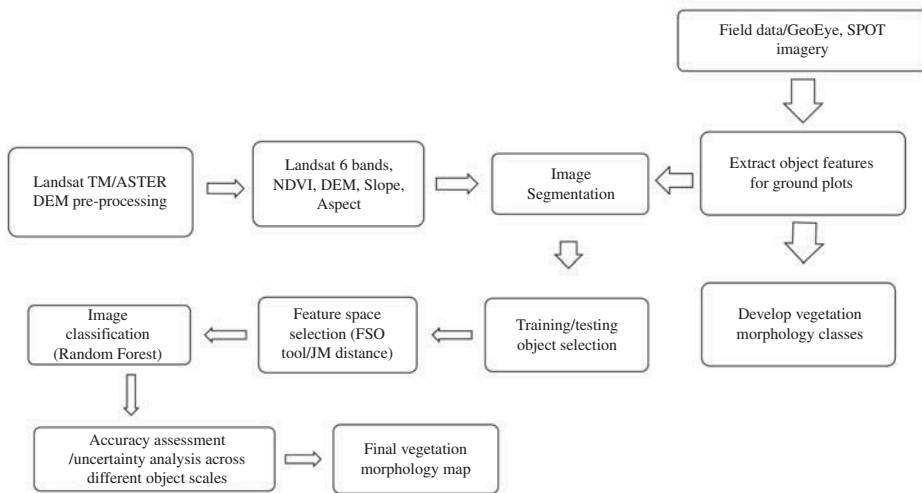


Figure 2. Schematic workflow of the study procedures.

Table 2. Segmentation parameters and associated object statistics for the six segmentation scales considered in the study.

Level	Scale parameter	Colour/shape	Smoothness/compactness	No. of Objects	Mean area of object (m <sup>2</sup> )
1	15	0.8/0.2	0.6/0.4	1,091,547	20,358
2	20	0.8/0.2	0.6/0.4	541,281	41,068
3	30	0.8/0.2	0.6/0.4	217,984	102,048
4	40	0.8/0.2	0.6/0.4	119,868	185,609
5	50	0.8/0.2	0.6/0.4	77,161	288,408
6	60	0.8/0.2	0.6/0.4	54,470	408,625

Figure 3 shows the segmentation results for a subset area at the six segmentation scales depicting how increasing segmentation scale value also increased the resulting object size. Visual inspection of segmentation results confirmed that beyond a scale value of 60, it was no longer possible to find representative homogeneous objects as the likelihood of class mixture within the object increased with object size (Liu and Xia 2010).

Hence, segmentation was not conducted beyond a scale value of 60. The other required segmentation parameters, shape and compactness, were kept at a constant value of 0.2 and 0.4, respectively (Table 2). These values were selected as optimal based on visual comparison of the results of several iterative segmentation runs. While conducting segmentation, the input Landsat bands, DEM, slope, and aspect were given equal weight while the NDVI layer was given higher weight compared with all other input layers.

### 3.3.2. Training/validation object selection

For each segmentation scale, training and test objects for classification were selected by (1) intersecting surrounding Landsat segments with specific field transects, and (2) more objects in the neighbourhood of field transect locations were selected as samples through interpreting and confirming their homogeneity in terms of vegetation physiognomy by overlying them on high-resolution imagery (GeoEye/SPOT) (Figure 4(a)). To ensure systematic geographic distribution of training/testing data, objects were divided between calibration and validation datasets based on the object ID created systematically across the image during segmentation. In most cases, sample objects derived with lower-scale values were nested within objects derived from higher factor values. In semi-arid savannas, the spatio-temporal pattern of rainfall determines the temporal dynamics of vegetation (Hill, Roman, and Schaaf 2011). Hence, the suitability of the selected training/testing objects was also validated by spatially overlaying them on the mean enhanced vegetation index (EVI) value calculated from six years (2005–2011) of MODIS data (MOD13Q1 product) (Figure 4(b)). Furthermore, to avoid the inclusion of any burned area in training/test data, the MODIS burned area product (MOD45A1) (Foster, Fluet, and Boose 1999) was used. Finally, for each scale, 843–1638 training/test objects with 68–631 objects per class were selected. Compared with other classes the number of samples selected for pan areas was higher because (1) many of the field tracks in central Kalahari follow the pan systems (Figure 1), allowing easier access, and (2) due to their high albedo it was relatively easier to visually distinguish pans on the high-spatial resolution imagery. Thus, while pans and bare area represent a relatively small percentage of the total study area, the number of validation and training samples selected for them was higher (Table 1).

### 3.3.3. Feature space selection for classification

For selection of optimal features to be used in classification, 41 spectral, shape, texture, pattern, and contextual features were initially selected to include a sufficiently wide range of features. To reduce the data dimensionality, Spearman's rank correlation analysis (Spearman 1904) was utilized to eliminate features with correlation coefficients above 0.9. Seventeen features were found to have correlations below this threshold value. The selection of best features from these remaining features was based on Jeffreys–Matusita distance (JM distance), which is a pair-wise measure of class separability based on the probability distribution of two classes. JM distance has a finite dynamic range that allows

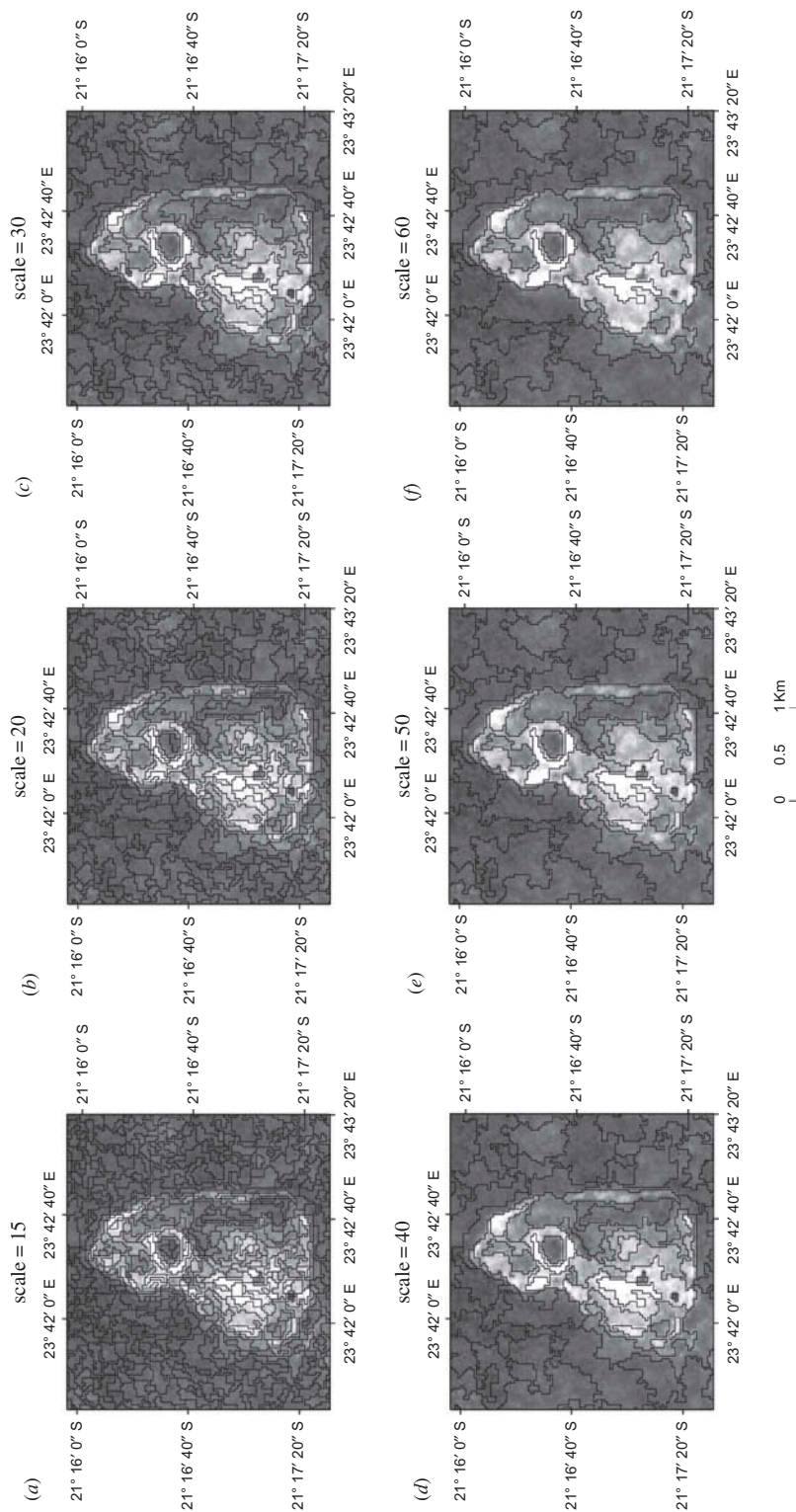


Figure 3. Illustration of change in object size with increasing scale factor in multi-resolution segmentation output.

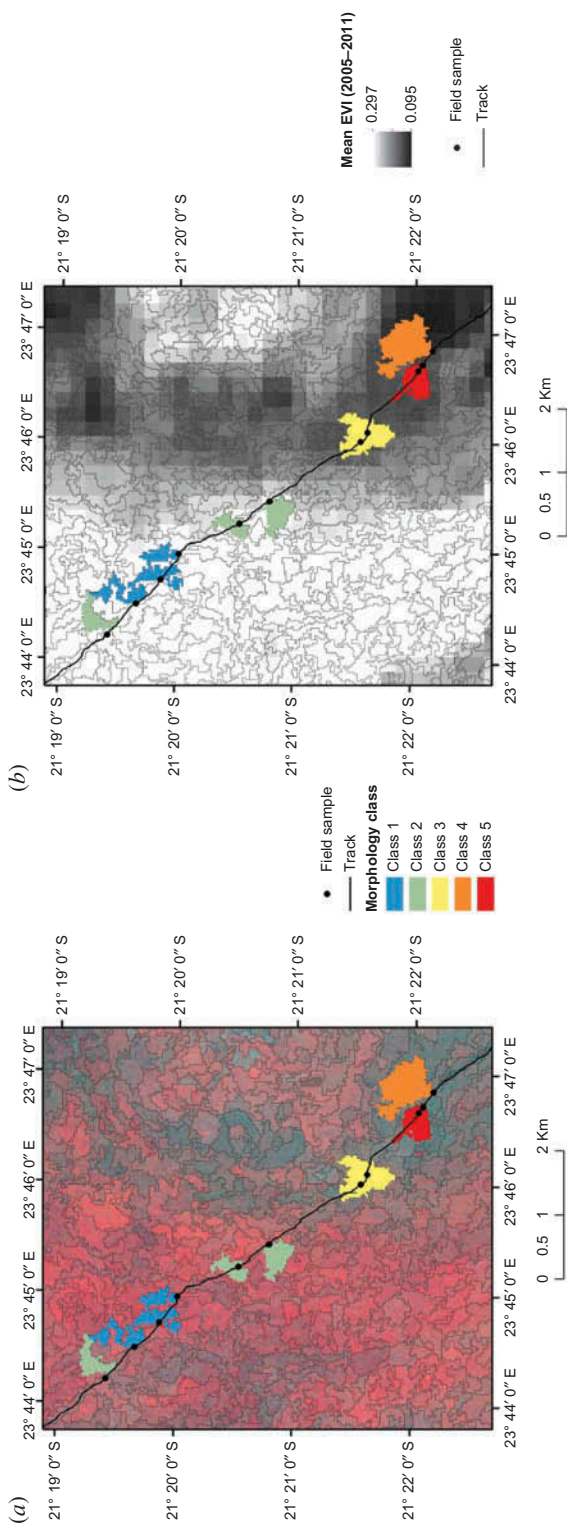


Figure 4. Example of the selection of training objects for different classes by intersecting location of field samples with homogeneous objects retrieved from segmentation. (a) Sample objects with Landsat false colour composite in the background; (b) background shows mean EVI values (2005–2011) derived from MODIS time-series images.

Table 3. Overview of the selected features that were used in final image classification.

Features	Description
Mean layer value	The mean value represents the mean brightness of an image object within a single band; used feature: Mean NDVI.
Ratios	The amount that a given band contributes to the total brightness; used feature: Ratio SWIR (Landsat TM band 6), Ratio NDVI.
Standard deviation	The standard deviation of all pixels which form an image object within a band; used feature: standard deviation aspect, standard deviation red, standard deviation green, standard deviation blue, standard deviation NIR, standard deviation GLCM (all bands).
Maximum difference	Minimum mean value of an object subtracted from its maximum value. The means of all bands belonging to an object are compared with each other and the result is divided by the brightness.
Texture after Haralick	GLCM (grey level co-occurrence matrix) calculated after Haralick, Shanmugam, and Dinstein (1973) describes how different combinations of pixel values occur within an object; used features (using the mean of all layers): GLCM contrast, GLCM dissimilarity, GLCM standard deviation. GLDV (grey level difference vector). The sum of the diagonals of the grey level co-occurrence matrix; used features (using the mean of all layers): GLDV Angular second moment.

easier comparison of class separability. For calculating JM distance, the SEATH tool was used (Nussbaum, Niemeyer, and Canty 2006; Marpu et al. 2008). Using the sample data for each class, a probability distribution is estimated based on mean and variance value. Thresholds are determined by fitting a Gaussian probability mixture model to the frequency distribution of a feature for the two classes. SEATH calculates class separability and threshold for every two-class combination. This study calculated the largest average JM distance (the mean of all two-class combinations) for every possible 9–17 feature combinations. Combinations with a lower number of features always had lower JM distance compared with those with more features, and selecting the lowest mean JM distance for the nine candidates was deemed unsuitable. Hence, the feature combination that resulted in the largest JM distance for the least separable pair of classes was selected, which is an approach followed in previous studies (Swain and Davis 1978; Turner 1989). This approach resulted in the final selection of 13 features (Table 3), of which four were textural features calculated after Haralick, Shanmugam, and Dinstein (1973). The appropriateness of these features was also confirmed by comparing them to results of feature space optimization (FSO), a feature selection tool available within eCognition (Loreau, Mouquet, and Holt 2003).

### 3.3.4. Image classification and accuracy assessment

In this study, vegetation morphology types were mapped using the non-parametric classifier, RF. The RF classifier builds multiple decision trees from bootstrap samples of the reference data. Decision-tree classifiers have advantages over traditional classifiers in that they make no assumptions about data distribution (e.g. normality) and can adapt to non-linear relationships inherent in the data (Friedl and Brodley 1997). RF classification has been employed in environmental remote sensing for a variety of applications including land-cover mapping (Pal 2005; Sesnie et al. 2008), forest structural parameters, biomass estimation (Baccini et al. 2004, Hudak et al. 2008), and mapping of invasive

species (Lawrence, Wood, and Sheley 2006). In land-cover mapping studies, RF classification has been found to yield overall accuracies that are either comparable to or better than other state-of-the-art classifiers such as neural networks and support vector machines (Pal 2005). In RF classification, each decision tree uses a random subset of training data and a random subset of input predictor variables, which reduces the correlation between decision trees as well as the overall computational complexity. Roughly 2/3 of the data are sampled with replacement while 1/3 are withheld from tree construction (also called 'out-of-the-bag' or OOB samples). OOB samples are used to calculate the difference between predicted *versus* observed samples based on which unbiased error matrix is calculated. Final class prediction is determined by majority voting based on the ensemble of trees. RF also calculates the measure of variable importance for individual classes and the classification as a whole. The variable importance measure allows determination of which of the input features contribute most to class separation. Predictor variable importance plots are generated based on a random permutation of the input variables, and the effect of the permutation is quantified for each variable by the change in the OOB error (Breiman 2001). Those variables important for separating classes show significant change in OOB error.

RF classification was implemented in the statistical package R using the 'randomForest' package (Liaw and Weiener 2002). The selected predictor objects were converted to ESRI shapefile and the associated attribute table was exported for RF classification in R. The parameters used for classification included: number of trees (ntree= 500), minimum samples in terminal node (nodesize = 10), and  $\sqrt{p}$  as the number of variables randomly sampled as candidates at each split, where  $p$  is the number of variables. After classification, the RF class predictions were written back to the attribute table. The classification accuracy was accessed using independent sample objects reserved for each class at each segmentation scale. Error matrices were calculated based on the number of objects per class without considering object size. Accuracy matrices reported include class-wise user's and producer's accuracy, overall accuracy, and kappa statistic at each segmentation scale.

## 4. Results and discussion

### 4.1. Vegetation morphology type mapping

The vegetation morphology type mapping in this study was based on a vegetation survey in the northern part of the Central Kalahari Game Reserve. In general, vegetation in the study area represents a transition zone between tree savanna with mixed broad-leaved and microphyllous (fine-leaved) species in the northern part that gradually changes to microphyllous species-dominated areas in the south and south-west. The mapped vegetation types for the whole study area are shown in Figure 5(a). Results show that vegetation morphology class 3 (i.e. mixed (40%–10%) medium-high shrubland with open, short herbaceous layer) was spatially the most dominant (covering about 60% of the area), whereas vegetation morphology class 1 (i.e. mixed deciduous woodland with shrubs and herbaceous layer) was least dominant (less than 1% of the total area). Vegetation morphology classes 2, 4, and 5 covered 20.32%, 13.76%, and 3.03% of the area, respectively. The spatial distribution of the different vegetation morphology types in the study area is a reflection of the spatial heterogeneity in the ecological mechanisms (e.g. soil characteristics, rainfall pattern, fire history) that influence savanna vegetation structure and composition. Vegetation morphology class 1 was present in the northern, northeastern, and



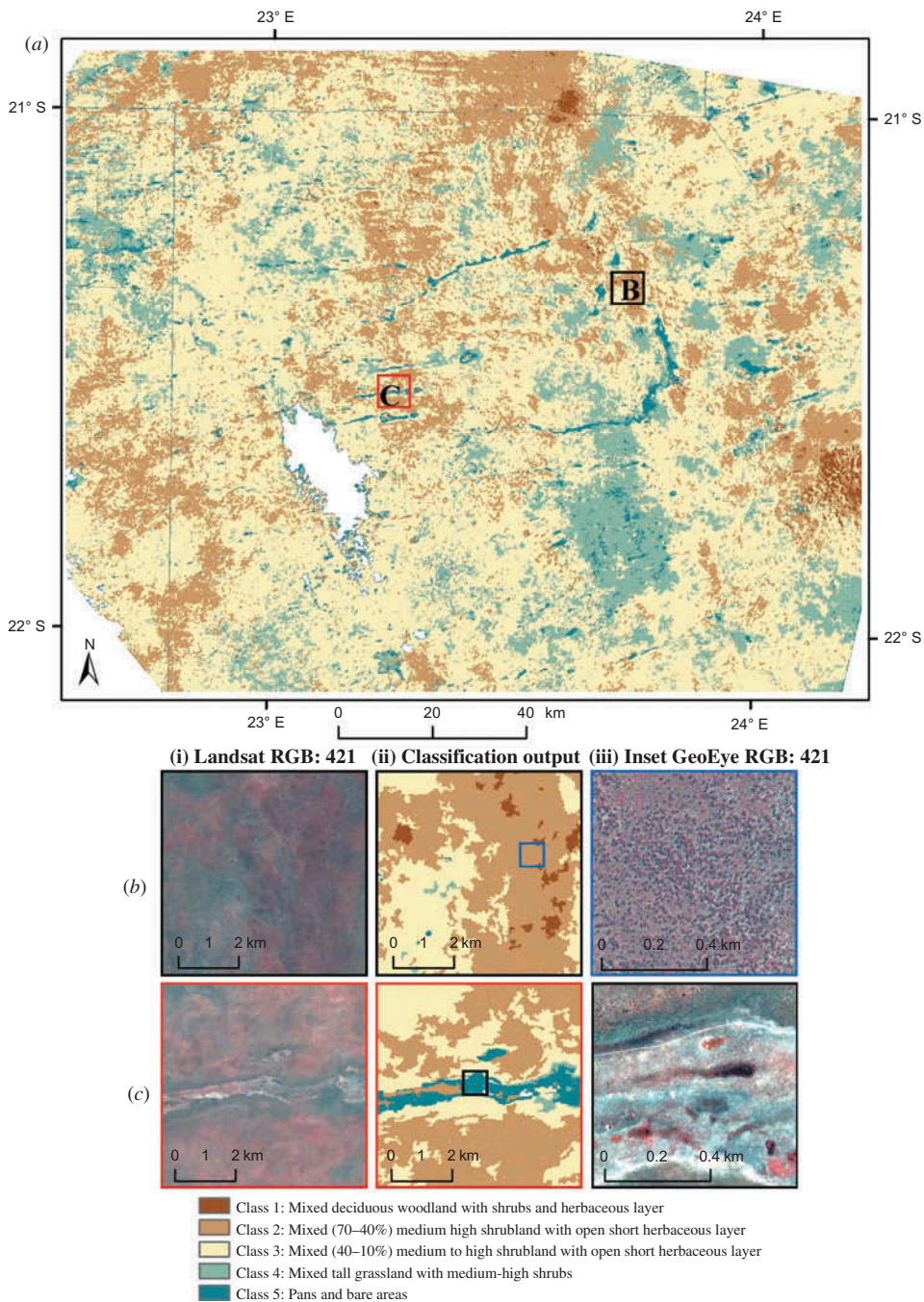


Figure 5. Vegetation morphology type classification derived from Random Forest classification on objects generated at segmentation scale value 40. Figure 5(a) shows a map of entire study area. Figures 5(b) and (c) show two subset areas with different morphology types and are compared to Landsat and GeoEye images.

southeastern parts of the study area (Figure 5(a)). During the field campaign, it was noted that the patches of vegetation morphology class 1 in the northern part of study area were dominated by *Terminalia prunioides* mixed with *Croton gratissimus* and *Acacia erioloba*. On the other hand, those in the south-eastern part of the study area were dominated by *Colophospermum mopane*, with *Lonchocarpus nelsii* and *Acacia luederitzii* co-dominant.

Vegetation morphology classes 1 and 2 generally dominate the area known as the northern Kalahari sandveld, which is topographically characterized by immobile longitudinal sand dunes. Vegetation morphology class 3 dominates areas that are topographically characterized as inter-dunal and plains with relatively shallow depth of sand. It also marks the transition zone between relatively densely vegetated areas and more open areas with predominantly herbaceous vegetation. Areas under vegetation morphology class 4 are mostly plains with shallow sand forming the top layer. Pan areas (vegetation morphology class 5) have dominant clay content and are found in the study area as either forming the ancient fossil river valley systems or others that are randomly scattered. Pan areas are characterized by the occasional occurrence of clumps of trees, also called 'tree islands', a result of the complex interaction of longer water availability, fire history, and soil characteristics.

#### 4.2. Class separability

Class spectral separability analysis was conducted on the training samples of the vegetation morphology classes studied using the 13 feature space variables finally selected. The separability metric used was JM distance, which indicates a relative measure of how reliably one class can be statistically separated compared with the remaining classes. The results of this separability analysis are reported in Table 4. Class pair-wise JM distance separability value is reported as being between 0–2, with 2 indicating complete separability. The result of pair-wise separability analysis suggested high separability for most class pairs. The lowest JM distance value was reported for the pairing of morphology classes 2 and 3 (i.e. JM distance, 1.61). This could be attributed to the fact that the differentiation between these two classes was established based on the percentage cover or shrub density as observed in the field and from high-resolution imagery. However, in feature space, the two classes were relatively similar even after using the optimally selected classification features. The highest inter-class separability values are reported for morphology class 5 and all other classes. This could be attributed to the very high surface albedo of pans and bare areas, and also to significant delay in the growing season period and late green-up caused by a typical flooding situation at the end of the rainy season. On the other hand, low class separability between morphology classes 2 and class 3 could be attributed to their comparative similarity in vegetation physiognomic characteristics.

Table 4. Jeffreys–Matusita distance class separability calculated for samples in the five vegetation morphology classes using the 13 features used in final classification.

	Class 1	Class 2	Class 3	Class 4	Class 5
Class 1	–	1.71	1.96	1.99	1.99
Class 2		–	1.61	1.82	1.99
Class 3			–	1.68	1.99
Class 4				–	1.98
Class 5					–

Table 5. User's, producer's, and average accuracy calculated for independent samples at six segmentation scale outputs.

Scale Class	15		20		30		40		50		60	
	users	prod	users	Prod	users	prod	users	prod	users	prod	users	prod
Class 1	86.31	83.65	87.65	83.71	86.9	80.88	83.67	79.07	83.01	75	79.71	71.07
Class 2	85.55	83.21	82.06	80.44	79.43	78.53	85.08	77.16	74.55	70.29	70.99	69.7
Class 3	80.43	76.81	84.13	81.03	85.78	90.45	88.33	89.58	85.13	87.93	84.77	86.58
Class 4	70	66.52	70.84	71.74	74.64	75.37	83.16	80.41	84.1	84.88	86.01	76.39
Class 5	93.01	90.7	94.51	90.59	95.29	88.51	95.03	92.24	95.94	92.2	91.8	89.44
Average accuracy	83.06	80.17	83.83	81.50	84.40	82.74	87.05	83.69	84.54	82.0	82.65	78.63
Kappa	0.76		0.79		0.81		0.82		0.81		0.79	

### 4.3. Segmentation scale versus classification accuracy

Results suggest that classification accuracy is sensitive to image segmentation scale, and various key outcomes were noted in this response. Among the six segmentation scales considered, the overall accuracy consistently increased from scale 15 to coarser scale values, attaining the highest overall accuracy at a segmentation scale of 40 (i.e. overall user's and producer's accuracy 87.05 and 83.69%, respectively; kappa = 0.82). However, at segmentation scales higher than 40, classification accuracy again decreased (Table 5). Furthermore, the observed sensitivity of classification accuracy to changing segmentation scale was also class specific, because the highest classification accuracy for different vegetation morphology classes was observed at different segmentation scales (Table 5). For example, areas with comparatively dense vegetation (e.g. morphology class 1) attained highest classification accuracy at the segmentation scale value of 15. In contrast, in areas dominated by relatively open herbaceous vegetation (e.g. morphology class 4), highest classification accuracy was observed at coarse segmentation scale values (i.e. 60). Unlike other classes, the classification accuracy of vegetation morphology class 5 (representing pans and bare areas) showed least variation and was less affected by change in segmentation scale (Table 5).

These results could be interpreted in the light of the spatial variability in the structural and functional properties of the different vegetation morphology types in the central Kalahari. The hierarchical segmentation approach used in this study is well suited for this purpose. Results indicate that the highest overall classification accuracy was not found at smaller segmentation scale values but at coarser ones. This could be attributed to the fact that at coarser scale values, integration of spectral signature across a large number of pixels increased the contrast among vegetation morphology types due to a reduction in within-class spectral variation (Strayer, Ewing, and Bigelow 2003). However, at more coarse segmentation scales (i.e. >40) the classification accuracy started to decrease, apparently due to reduction in spectral contrast between classes due to class mixing. Savannas are often considered patch-dynamic systems because the vegetation spatial distribution resembles patchy shapes due to the influence of determinants such as high spatio-temporal variability in rainfall pattern and fire history (Moustakas et al. 2009). For accurately characterizing vegetation morphology in savannas, it is important that segmentation output matches patch size and structure for different classes of interest prior to classification (Gustafson 1998; Tallmon et al. 2003). This study compared segmentation output using six different scale values. Although the highest overall classification

accuracy was achieved at the scale value of 40, for different classes the highest class-specific accuracies were achieved at different segmentation scale values. Thus, no single scale values can be suggested as optimal for all classes. The optimal segmentation scale (for which a given class attains highest classification accuracy) for vegetation morphology class 1 was lower (i.e. 15) than for class 4, which attained the highest classification accuracy at a larger segmentation scale (i.e. 50). These results could be attributed to the fact that while patches of vegetation morphology class 1 are relatively small and woody and occupy different longitudinal dune systems both topographically and pedologically, vegetation morphology class 4 includes predominant herbaceous life forms that occupy inter-dunal areas as well as plains that cover larger areas, with larger patch size. In contrast, the classification accuracy of vegetation morphology class 5 (i.e. pans and bare areas) was not sensitive to change in segmentation scale and was mapped with high accuracy across all segmentation scales tested (Table 5). These results highlight that segmented objects for pan and bare areas have low within-class spectral variability compared with other classes, and are relatively homogeneous.

#### 4.4. Variable importance of RF classification

Due to the availability of hundreds of feature space variables under the OBIA approach, analysis can be very time consuming in terms of image processing and memory allocation. Hence, selecting suitable feature space variables is critical for conducting OBIA-based analysis over large geographical areas. This study highlights the most useful feature space variables for mapping vegetation morphology types in dry savanna systems. Many of the initial geometrical and contextual features were found to be highly correlated with each other and were subsequently omitted. Based on the feature selection criteria explained in Section 3, finally 13 features were selected for classification. Figure 6 depicts the class-specific as well as the overall importance score of 13 variables for the classification obtained at a segmentation scale value of 40 (for which highest overall classification accuracy was observed). The variable importance plot depicts these 13 features in order of decreasing importance for discriminating vegetation morphology type. Figures 6(a)–(e) show class-specific variable importance while the overall variable importance is depicted in Figure 6(f). Standard deviation of mid-infrared was the most important feature variable, underscoring the distinguishability of savanna vegetation morphology types in a pedological context. This result confirms the findings of previous studies based mainly on field observation, emphasizing the subjacent soil properties as an important determinant of savanna structure in the central Kalahari (van Rooyen and van Rooyen 1998; Fagan 2002). The presence of two texture-associated variables (grey-level co-occurrence matrix (GLCM) contrast and GLCM standard deviation) among the top five variables (and total of four texture-related variables among the 13 selected variables) shows the importance of textural features in discriminating savanna vegetation morphology. These results suggest that semi-arid systems, where different vegetation morphology types lead to subtle differences in physiognomic characteristics, may exhibit a similar spectral response and require inclusion of textural characteristics for effective discrimination. The class-specific variable importance indicates the suitability of each feature for an increase in accuracy in the random forest ensemble. For all classes the most significant classification feature was spectral (i.e. mean NDVI or ratio NDVI), except for vegetation morphology class 4 for which textural feature was the most significant (i.e. GLCM standard deviation).

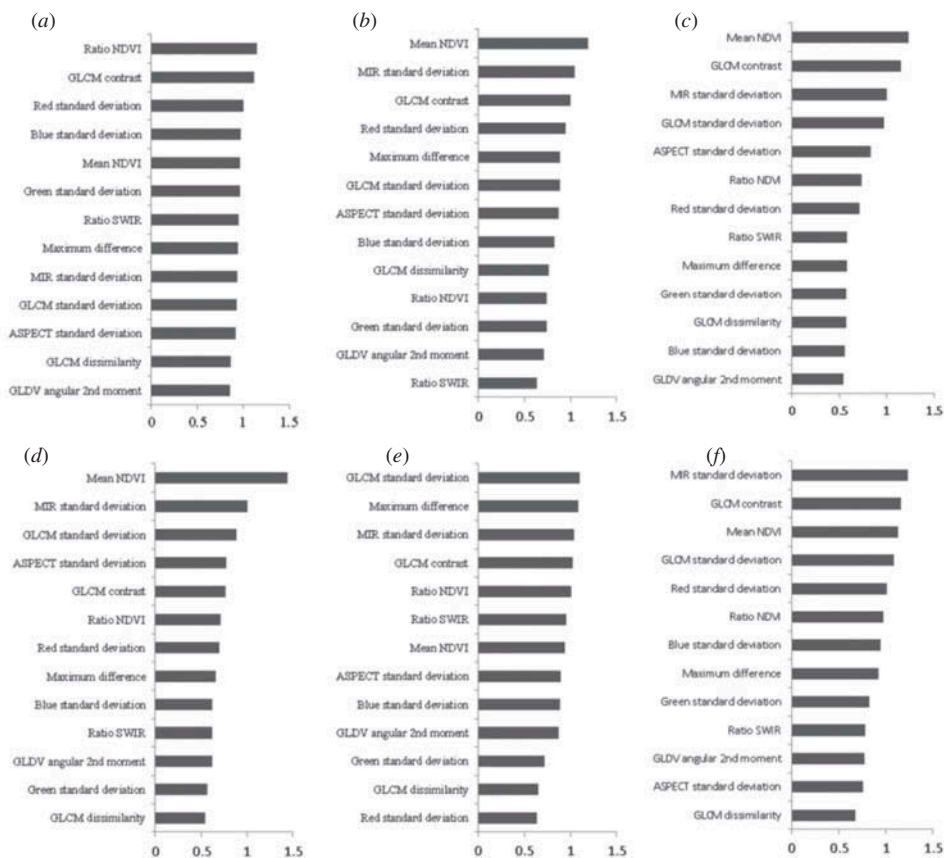


Figure 6. Variable importance reported as mean decrease in class-specific and overall producer’s accuracy from 500 trees in Random Forest classification. Those variables with higher mean decrease in accuracy are considered to be more important for overall or class-level classification. Figures (a)–(e) represent class-specific variable importance for morphology classes 1–5, respectively, and (f) depicts variable importance for overall classification. All results are for classification conducted for objects generated at segmentation scale 40. In each figure, the x-axis represents percentage decrease in accuracy and the y-axis represents the variable name.

### 5. Conclusions

This study represents an application of OBIA for mapping vegetation morphology types at landscape scale in an extensive and structurally heterogeneous semi-arid savanna ecosystem. The objective was to accurately map the vegetation morphology types in the central Kalahari by determining the optimal segmentation scale and best features for classification. Results showed that the highest overall classification accuracy was recorded not at the finest segmentation scale but at coarser scales. Furthermore, for different classes, highest class-specific accuracy was achieved at different segmentation scales, highlighting the fact that spatial heterogeneity in savanna systems requires multi-scale characterization. The hierarchical OBIA approach adapted in this study was found to be suitable for this purpose. This approach treats landscapes as relatively homogeneous mosaics of patches that allow smoothing of local variability and enhancement of class separability. This

approach is especially relevant in the semi-arid savanna systems with low niche differentiation and where the complex interaction of biotic and abiotic determinants often results in landscapes that should be treated as patches. Furthermore, the multi-scale hierarchical approach was deemed suitable because in natural landscapes such as savanna the optimal patch size for different morphology types is often unknown and is expected to have a multi-scale character. Besides the spectral features, object-level texture features were also found to be important for distinguishing savanna vegetation morphology types. This could be attributed to the fact that vegetation morphology types in semi-arid systems are often marked by subtle difference in vegetation physiognomy, and species composition has relatively similar spectral characteristics. Texture information is based on second order statistics and provides the dimensionality needed for distinguishing these subtle differences between classes.

The RF classification technique used in this study proved to be effective in terms of classification error, overfitting, and variable importance measures. The bottom-up approach of using *in situ*-derived vegetation physiognomic properties to derive classification samples that could be coupled to advance classification techniques holds promise for remote-sensing applications in savanna systems. The highest overall classification accuracy of 85.59% obtained at segmentation scale 40 was satisfactory for mapping vegetation morphology types in semi-arid savanna, given the subtle physiognomic difference for several classes. This study showed that *in situ* information combined with OBIA–RF classification of multispectral imagery can be an effective method for mapping vegetation morphology classes in semi-arid savanna systems at the landscape scale. The approach allowed the evaluation and selection of several spectral, geometrical, contextual, and textural features, and finally determination of a suitable analysis scale. The vegetation morphology map created in this study is significant and provides the necessary environmental geodata for the study area. It is expected to support a variety of ecological studies such as understanding the spatio-temporal dynamics of habitat use by the wildlife, plant function, and biogeochemical fluxes, and overall management of the area. The mapped spatial distribution of vegetation morphology types may also serve as useful input to models of climate and land-use change in the study area. This study can map vegetation morphology types defined on the basis of vegetation physiognomic characteristics rather than floristic/species aspects. Therefore, future related research should focus on applying this technique to distinguish floristic classes in semi-arid savannas using both medium-resolution (e.g. Landsat) and high-resolution imagery (e.g. GeoEye).

### Acknowledgements

We would like to thank Thoralf Meyer and Glyn Maude for field work planning and logistical support; Kevin MacFarlane, Moses Selebesto and field assistants for help during field campaigns; and Mario Cardozo and Gargi Chaudhuri for discussions that helped improve this work. The authors also thank the anonymous reviewers for their valuable comments that helped refine the manuscript.

### Funding

This research was supported by National Science Foundation: Doctoral Dissertation Improvement [grant number 1203580] and a Veselka field research grant from University of Texas at Austin. GeoEye and SPOT images were provided as an imagery grant from the GeoEye Foundation and Planet Action/Austrim, respectively.

## References

- Baccini, A., M. A. Friedl, C. E. Woodcock, and R. Warbington. 2004. "Forest Biomass Estimation Over Regional Scales Using Multisource Data." *Geophysical Research Letters* 31: L10501.
- Benz, U. C., P. Hofmann, G. Willhauck, I. Lingenfelder, and M. Heynen. 2004. "Multi-Resolution, Object-Oriented Fuzzy Analysis of Remote Sensing Data for GIS-Ready Information." *ISPRS Journal of Photogrammetry and Remote Sensing* 58: 239–258.
- Blaum, N., E. Rossmanith, and F. Jeltsch. 2007. "Land Use Affects Rodent Communities in Kalahari Savannah Rangelands." *African Journal of Ecology* 45: 189–195.
- Breiman, L. 2001. "Random Forests." *Machine Learning* 45: 5–32.
- Cramer, W., A. Bondeau, F. I. Woodward, I. C. Prentice, R. A. Betts, V. Brovkin, P. M. Cox, V. Fisher, J. A. Foley, A. D. Friend, C. Kucharik, M. R. Lomas, N. Ramankutty, S. Sitch, B. Smith, A. White, and C. Young-Molling. 2001. "Global Response of Terrestrial Ecosystem Structure and Function to CO<sub>2</sub> and Climate Change: Results From Six Dynamic Global Vegetation Models." *Global Change Biology* 7: 357–373.
- Davidson, E. A., G. P. Asner, T. A. Stone, C. Neill, and R. O. Figueiredo. 2008. "Objective Indicators of Pasture Degradation From Spectral Mixture Analysis of Landsat Imagery." *Journal of Geophysical Research-Biogeosciences* 113: 7.
- Dougill, A., and N. Trodd. 1999. "Monitoring and Modelling Open Savannas Using Multisource Information: Analyses of Kalahari Studies." *Global Ecology and Biogeography* 8: 211–221.
- Dougill, A. J., D. S. G. Thomas, and A. L. Heathwaite. 1999. "Environmental Change in the Kalahari: Integrated Land Degradation Studies for Nonequilibrium Dryland Environments." *Annals of the Association of American Geographers* 89: 420–442.
- Elmore, A. J., J. F. Mustard, S. J. Manning, and D. B. Lobell. 2000. "Quantifying Vegetation Change in Semi-arid Environments: Precision and Accuracy of Spectral Mixture Analysis and the Normalized Difference Vegetation Index." *Remote Sensing of Environment* 73: 87–102.
- Fagan, W. F. 2002. "Connectivity, Fragmentation, and Extinction Risk in Dendritic Metapopulations." *Ecology* 83: 3243.
- Foster, D. R., M. Fluet, and E. R. Boose. 1999. "Human or Natural Disturbance: Landscape-Scale Dynamics of the Tropical Forests of Puerto Rico." *Ecological Applications* 9: 555.
- Friedl, M. A., and C. E. Brodley. 1997. "Decision Tree Classification of Land Cover From Remotely Sensed Data." *Remote Sensing of Environment* 61: 399–409.
- Giri, C., Z. L. Zhu, and B. Reed. 2005. "A Comparative Analysis of the Global Land Cover 2000 and MODIS Land Cover Data Sets." *Remote Sensing of Environment* 94: 123–132.
- Groffman, P. M., J. S. Baron, T. Blett, A. J. Gold, and I. Goodman. 2005. "Ecological Thresholds: The Key to Successful Environmental Management or an Important Concept with No Practical Application." *Ecosystem* 9: 1–13.
- Groffman, P. M., T. M. Tiedje, D. L. Mokma, and S. Simkins. 1992. "Regional-Scale Analysis of Denitrification in North Temperate Forest Soils." *Landscape Ecology* 7: 45–54.
- Gustafson, E. J. 1998. "Quantifying Landscape Spatial Pattern: What Is the State of the Art." *Ecosystem* 1: 143–156.
- Haralick, R. M., K. Shanmugam, and I. H. Dinstein. 1973. "Textural Features for Image Classification." *Systems, Man and Cybernetics, IEEE Transactions on* 6: 610–621.
- Hill, M. J., M. O. Roman, and C. B. Schaaf. 2011. "Biogeography and Dynamics of Global Tropical and Subtropical Savannas: A Spatiotemporal View." In *Ecosystem Function in Savannas: Measurement and Modelling at Landscape to Global Scales*, edited by M. J. Hill and N. P. Hanan, 3–37. Boca Raton, FL: CRC Press.
- Hudak, A. T., N. L. Crookston, J. S. Evans, D. E. Hall, and M. J. Falkowski. 2008. "Nearest Neighbor Imputation of Species-Level, Plot-Scale Forest Structure Attributes From LiDAR Data." *Remote Sensing of Environment* 112: 2232–2245.
- Huete, A. R., and R. D. Jackson. 1988. "Soil and Atmosphere Influences on the Spectra of Partial Canopies." *Remote Sensing of Environment* 25: 89–105.
- Huete, A. R., R. D. Jackson, and D. F. Post. 1985. "Spectral Response of a Plant Canopy with Different Soil Backgrounds." *Remote Sensing of Environment* 17: 37–53.
- Jules, E. S., M. J. Kauffman, W. D. Ritts, and A. L. Carroll. 2002. "Spread of an Invasive Pathogen Over a Variable Landscape: A Nonnative Root Rot on Port Orford Cedar." *Ecology* 83: 3167–3181.

- Keyghobadi, N., J. Roland, and C. Strobeck. 1999. "Influence of Landscape on the Population Genetic Structure of the Alpine Butterfly *Parnassius smintheus* (Papilionidae)." *Molecular Ecology* 8: 1481–1495.
- Knight, T. W., and D. W. Morris. 1996. "How Many Habitats Do Landscapes Contain?" *Ecology* 77: 1756–1764.
- Laliberte, A. S., A. Rango, K. M. Havstad, J. F. Paris, R. F. Beck, R. Mcneely, and A. L. Gonzalez. 2004. "Object-Oriented Image Analysis for Mapping Shrub Encroachment From 1937 to 2003 in Southern New Mexico." *Remote Sensing of Environment* 93: 198–210.
- Latifovic, R., and I. Olthof. 2004. "Accuracy Assessment Using Sub-Pixel Fractional Error Matrices of Global Land Cover Products Derived From Satellite Data." *Remote Sensing of Environment* 90: 153–165.
- Lawrence, R. L., S. D. Wood, and R. L. Sheley. 2006. "Mapping Invasive Plants Using Hyperspectral Imagery and Breiman Cutler Classifications (RANDOMFOREST)." *Remote Sensing of Environment* 100: 356–362.
- Liaw, A., and M. Weiener. 2002. "Classification and Regression by Random Forest." *R News* 2: 18–22.
- Liu, D. S., and F. Xia. 2010. "Assessing Object-Based Classification: Advantages and Limitations." *Remote Sensing Letters* 1: 187–194.
- Loreau, M., N. Mouquet, and R. D. Holt. 2003. "Meta-Ecosystems: A Theoretical Framework for a Spatial Ecosystem Ecology." *Ecology Letters* 6: 673–679.
- Makhabu, S. W., B. Marotsi, and J. Perkins. 2002. "Vegetation Gradients Around Artificial Water Points in the Central Kalahari Game Reserve of Botswana." *African Journal of Ecology* 40: 103–109.
- Marpu, P. R., S. Nussbaum, I. Niemeyer, and R. Gloaguen. 2008. "A Procedure for Automatic Object-Based Classification." In *Object-Based Image Analysis Spatial Concepts for Knowledge-Driven Remote Sensing Applications. Series: Lecture Notes in Geoinformation and Cartography*, edited by T. Blaschke, S. Lang, and G. Hay, 169–184. Berlin: Springer.
- Mishra, N. B., and K. A. Crews. 2013. "Estimating Fractional Land Cover in Semi-arid Central Kalahari: The Impact of Mapping Method (Spectral Unmixing Versus Object-based Image Analysis) and Vegetation Morphology." *Geocarto International*. doi:10.1080/10106049.2013.868041.
- Mishra, N. B., K. A. Crews, and G. S. Okin. under review. "Relating Spatial Patterns of Fractional Land Cover to Savanna Vegetation Morphology using Multi-scale Remote Sensing in the Central Kalahari." *International Journal of Remote Sensing*.
- Mistry, J. 2000. "Savannas." *Progress in Physical Geography* 24: 601–608.
- Moustakas, A., K. Sakkos, K. Wiegand, D. Ward, K. M. Meyer, and D. Eisinger. 2009. "Are Savannas Patch-Dynamic Systems? a Landscape Model." *Ecological Modelling* 220: 3576–3588.
- Naiman, R. J., and K. H. Rogers. 1997. "Large Animals and System Level Characteristics in River Corridors." *BioScience* 47: 521–529.
- Newton, A. C., R. A. Hill, C. Echeverria, D. Golicher, J. M. R. Benayas, L. Cayuela, and S. A. Hinsley. 2009. "Remote Sensing and the Future of Landscape Ecology." *Progress in Physical Geography* 33: 528–546.
- Nussbaum, S., I. Niemeyer, and M. J. Canty. 2006. "SEaTH – A New Tool for Automated Feature Extraction in the Context of Object-Oriented Image Analysis." In *Proceedings of the 1st International Conference on Object-based Image Analysis (OBIA 2006)*, ISPRS 36 (4): C42, July.
- Okin, G. S., D. A. Roberts, B. Murray, and W. J. Okin. 2001. "Practical Limits on Hyperspectral Vegetation Discrimination in Arid and Semi-arid Environments." *Remote Sensing of Environment* 77: 212–225.
- Opdam, P., R. Foppen, and C. Vos. 2002. "Bridging the Gap Between Ecology and Spatial Planning in Landscape Ecology." *Landscape Ecology* 16: 767–779.
- Pal, M. 2005. "Random Forest Classifier for Remote Sensing Classification." *International Journal of Remote Sensing* 26: 217–222.
- Pearson, S. M., M. G. Turner, and J. B. Drake. 1999. "Landscape Change and Habitat Availability in the Southern Appalachian Highlands and the Olympic Peninsula." *Ecological Application* 9: 1288–1304.



- Ringrose, S., W. Matheson, P. Wolski, and P. Huntsman-Mapila. 2003. "Vegetation Cover Trends Along the Botswana Kalahari Transect." *Journal of Arid Environments* 54: 297–317.
- Scholes, R. J., P. R. Dowty, K. Caylor, D. A. B. Parsons, P. G. H. Frost, and H. H. Shugart. 2002. "Trends in Savanna Structure and Composition Along an Aridity Gradient in the Kalahari." *Journal of Vegetation Science* 13: 419–428.
- Scholes, R. J., and B. H. Walker. 1993. *An African Savanna: Synthesis of the Nylsvley Study*. Cambridge: Cambridge University Press.
- Schwartz, M. K., L. S. Mills, Y. Ortega, L. F. Ruggiero, and F. W. Allendorf. 2003. "Landscape Location Affects Genetic Variation of Canada Lynx (*Lynx Canadensis*)." *Molecular Ecology* 12: 1807–1816.
- Seagle, S. W. 2003. "Can Deer Foraging in Multiple-Use Landscapes Alter Forest Nitrogen Budgets." *Oikos* 103: 230–234.
- Sesnie, S. E., P. E. Gessler, B. Finegan, and S. Thessler. 2008. "Integrating Landsat TM and SRTM-DEM Derived Variables with Decision Trees for Habitat Classification and Change Detection in Complex Neotropical Environments." *Remote Sensing of Environment* 112: 2145–2159.
- Skarpe, C. 1990. "Shrub Layer Dynamics Under Different Herbivore Densities in an Arid Savanna, Botswana." *Journal of Applied Ecology* 27: 873–885.
- Soranno, P. A., K. E. Webster, J. L. Riera, T. K. Kratz, and J. S. Baron. 1999. "Spatial Variation Among Lakes Within Landscapes: Ecological Organization Along Lake Chains." *Ecosystem* 2: 395–410.
- Spearman, C. 1904. "The Proof and Measurement of Association Between Two Things." *American Journal of Psychology* 15: 72–101.
- Spies, T. A., W. J. Ripple, and G. A. Bradshaw. 1994. "Dynamics and Pattern of a Managed Coniferous Forest Landscape in Oregon." *Ecological Application* 4: 555–568.
- Steffan-Dewenter, I., U. Munzenberg, C. Burger, C. Thies, and T. Tscharntke. 2002. "Scale-Dependent Effects of Landscape Context on Three Pollinator Guilds." *Ecology* 83: 1421–1432.
- Strayer, D. L., R. E. Beighley, L. C. Thompson, A. Brooks, and C. Nilsson. 2003. "Effects of Land Cover on Stream Ecosystems: Roles of Empirical Models and Scaling Issues." *Ecosystem* 6: 407–423.
- Strayer, D. L., H. A. Ewing, and S. Bigelow. 2003. "What Kind of Spatial and Temporal Details Are Required in Models of Heterogeneous Systems." *Oikos* 102: 654–662.
- Swain, H., and S. M. Davis. 1978. *Remote Sensing: The Quantitative Approach*. New York: McGraw-Hill.
- Tallmon, D. A., E. S. Jules, N. J. Radke, and L. S. Mills. 2003. "Of Mice and Men and Trillium: Cascading Effects of Forest Fragmentation." *Ecological Application* 13: 1193–1203.
- Tangestani, M. H., N. Mazhari, B. Agar, and F. Moore. 2008. "Evaluating Advanced Spaceborne Thermal Emission and Reflection Radiometer (ASTER) Data for Alteration Zone Enhancement in a Semi-Arid Area, Northern Shahr-e-Babak, SE Iran." *International Journal of Remote Sensing* 29: 2833–2850.
- Tews, J., N. Blaum, and F. Jeltsch. 2004. "Structural and Animal Species Diversity in Arid and Semi-Arid Savannas of the Southern Kalahari." *Annals of Arid Zone* 42: 1–13.
- Thomas, D. S. G., and D. Sporton. 1997. "Understanding the Dynamics of Social and Environmental Variability: The Impacts of Structural Land Use Change on the Environment and Peoples of the Kalahari, Botswana." *Applied Geography* 17: 11–27.
- Thomas, D. S. G., and C. Twyman. 2004. "Good or Bad Rangeland? Hybrid Knowledge, Science, and Local Understandings of Vegetation Dynamics in the Kalahari." *Land Degradation & Development* 15: 215–231.
- Trzcinski, M. K., L. Fahrig, and G. Merriam. 1999. "Independent Effects of Forest Cover and Fragmentation on the Distribution of Forest Breeding Birds." *Ecological Application* 9: 586–593.
- Turner, M. G. 1989. "Landscape Ecology: The Effect of Pattern on Process." *Annual Review of Ecological and Systematic* 20: 171–197.
- Turner, M. G. 2005. "Landscape Ecology in North America: Past, Present and Future." *Ecology* 86: 1967–1974.
- Turner, M. G., S. M. Pearson, P. Bolstad, and D. N. Wear. 2003. "Effects of Land-Cover Change on Spatial Pattern of Forest Communities in the Southern Appalachian Mountains (USA)." *Landscape Ecology* 18: 449–464.

- Turner, M. G., W. H. Romme, R. H. Gardner, R. V. O'neill, and T. K. Kratz. 1993. "A Revised Concept of Landscape Equilibrium: Disturbance and Stability on Scaled Landscapes." *Landscape Ecology* 8: 213–227.
- Turner, M. G., D. B. Tinker, W. H. Romme, D. M. Kashian, and C. M. Litton. 2004. "Landscape Patterns of Sapling Density, Leaf Area, and Aboveground Net Primary Production in Postfire Lodgepole Pine Forests, Yellowstone National Park (USA)." *Ecosystem* 7: 751–775.
- Urban, D., S. Goslee, K. Pierce, and T. Lookingbill. 2002. "Extending Community Ecology to Landscapes." *Ecoscience* 9: 200–202.
- Van Rooyen, N., D. Bezuidenhout, G. K. Theron, and J. D. P. Bothma. 1990. "Monitoring of the Vegetation Around Artificial Watering Points (Windmills) in the Kalahari Gemsbok National Park." *Koedoe* 33: 63–88.
- Van Rooyen, N., and M. W. Van Rooyen. 1998. "Vegetation of the South-Western Arid Kalahari: An Overview." *Transactions of the Royal Society of South Africa* 53: 113–140.
- Werger, M. J. A. 1973. "Notes on the Phytogeographical Affinities of the Southern Kalahari." *Bathalia* 11: 177–180.
- Wiegand, K., D. Saltz, and D. Ward. 2006. "A Patch-Dynamics Approach to Savanna Dynamics and Woody Plant Encroachment – Insights From an Arid Savanna." *Perspectives in Plant Ecology, Evolution and Systematics* 7: 229–242.
- Wu, J., and D. Marceau. 2002. "Modelling Complex Ecological Systems: An Introduction." *Ecological Modelling* 153: 1–6.
- Xie, Y. C., Z. Y. Sha, and M. Yu. 2008. "Remote Sensing Imagery in Vegetation Mapping: A Review." *Journal of Plant Ecology-UK* 1: 9–23.
- Yu, Q., P. Gong, N. Clinton, G. Biging, M. Kelly, and D. Schirokauer. 2006. "Object-Based Detailed Vegetation Classification. with Airborne High Spatial Resolution Remote Sensing Imagery." *Photogrammetric Engineering and Remote Sensing* 72: 799–811.